the resistivity anisotropy and this explains that the transverse magnetoresistance was found negative for Tb, Dy, and Ho and positive for Er.

We have reported in this Letter the observation of the resistivity anisotropy of dilute magnetic impurities (to our knowledge this is the first clear observation of such an effect). This effect is interesting because it should give information on the coupling of conduction electrons with the quadrupolar moment of RE impurities and also because it should be very sensitive to the CEF structure. Similar experiments for transition impurities would also be of interest, as they could provide evidence of small orbital contributions to the magnetic moment.

We thank J. Sierro (University of Geneva) and A. P. Murani (Imperial College) who furnished many of the alloys that we have studied.

*Associé au Centre National de la Recherche Scientifique.

[1]J. Kondo, Progr. Theor. Phys. 27, 772 (1962).

[2]For RE impurities in a noble metal it is more correct to take instead of $V\hat{o}(r)$ a potential $P_2(\cos\theta_{kk'})V_2$ which expresses a d-resonant scattering ($5d$ nonmagnetic virtual bound state). This changes the expression (4) for the anisotropy slightly.

[3]T. Van Peski Tinbergen and A. J. Dekker, Physica (Utrecht) 29, 917 (1963).

[4]A. Friederich and A. Fert, to be published.

[5]A. Fert, J. Phys. F: Met. Phys. 3, 2126 (1973).

[6]G. de Vries and J. Bijvoet, J. Appl. Phys. 39, 797 (1968).

Deuterium Lattice Location in Cr and W†

S. T. Picraux and F. L. Vook
Sandia Laboratories, Albuquerque, New Mexico 87115
(Received 20 May 1974)

Direct determination of the lattice location of implanted deuterium in single-crystal chromium has been made for the first time. Ion-channeling measurements of the angular distributions along the ⟨100⟩ axial and {100} planar directions indicate that implanted D occupies the octahedral position in bcc Cr. This contrasts to the expected tetrahedral interstitial position recently observed under the same conditions for bcc W. These results further clarify the apparent anomaly in the thermodynamic data for hydrogen solubility in Cr.

Fundamental structural information for hydrogen in transition metals is particularly important because of the great theoretical and technological interest. The low solubility of hydrogen in chromium and tungsten (group VI B) has prevented previous measurements of the lattice location of hydrogen by the usual technique of neutron diffraction. Recently ion channeling has been applied to studies of the lattice location of hydrogen in single-crystal metals.[1,2] The first lattice-location data for deuterium in W have been obtained by combining ion implantation with ion channeling and nuclear-reaction analysis.[2] These results showed that the implanted deuterium resides in the tetrahedral interstitial site, which is the expected site in bcc metals. The absence of any lattice-location data for hydrogen in Cr and the apparent inconsistency in the thermodynamic results for hydrogen solubility in Cr relative to other bcc and close-packed metals[3] suggested that the hydrogen lattice location in bcc Cr could be other than the expected tetrahedral site.

This Letter presents the first lattice-location data for hydrogen in Cr and shows that implanted D occupies the octahedral interstitial site and not the tetrahedral site previously found for implanted D in W. The results provide a direct comparison of the lattice location of D in Cr and W by the same technique and indicate anomalous high-temperature hydrogen-solubility behavior of Cr relative to the other bcc metals.[3]

The ⟨100⟩-oriented single crystals of 99.995% pure Cr and 99.999% pure W were obtained from Metals Research and from Materials Research, respectively. The D was introduced by ion implantation into the ⟨100⟩ faces of Cr and W samples along a nonchanneling direction 7° from the ⟨100⟩ axis. The 15- and 30-keV D^+ ion implantations were made, respectively, into the Cr and W samples by accelerating the molecular species D_3^+ at a factor of 3 higher energy. Implants were performed at 296 K to fluences of 3×10^{15} D atoms/

cm^2. The projected range for 15-keV D^+ in Cr is 1140 Å and for 30-keV D^+ in W is 1270 Å.[4]

Ion-channeling analysis was performed with incident 750-keV ^3He ions by monitoring the ion backscattering from the Cr and W, and by using the nuclear reaction $D(^3He,p)^4He$ to monitor the implanted D. This nuclear reaction has a Q value of 18.3 MeV and a peak cross section ~70 mb/sr at a ^3He beam energy of ~650 keV. A 300-mm^2 surface-barrier detector with 500-μm depletion depth was located at a scattering angle $\approx 135°$ with a solid angle ≈ 0.1 sr.

Angular collimation of the incident beam resulted in an angular divergence (full angle) $\leq 0.06°$ and the angular resolution of the goniometer was 0.01°. Single-channel analyzers were set to accept the Cr and W signals from depths corresponding to the ranges of the implanted impurity. Further details of the technique can be found in Ref. 2.

Angular channeling results for ⟨100⟩ scans of implanted D in Cr and W are shown in Fig. 1. The backscattering and nuclear-reaction yields have been normalized by the random (nonchanneled) yields. The random levels indicated by the dashed lines at 1.0 correspond, respectively, to ~4000 and ~14 500 counts for scattering from Cr and W, and 610 and 180 counts for the reaction yield from D in Cr and W. The low backscattering minimum yields of 1.7 and 1.1% for the ⟨100⟩ axis in Cr and W, respectively, observed prior to implantation, indicate good crystalline quality. For W the strong enhancement in the D yield (flux peak) is seen with a full angular width of 0.2° and a maximum relative yield of 1.8, whereas the W channeling critical angle is observed to be 2.01°. In contrast to W (where the D yield does not drop below the random level), the ⟨100⟩ data for Cr show a sharp flux peak with maximum relative D yield of ≈ 1.3 and width $\approx 0.3°$ superimposed on a broad dip with minimum relative D yield of ≈ 0.73. The angular width of the D dip of $\approx 1.4°$ is similar to that observed for the Cr of 1.38°. The yields and angular widths for Cr and W suggest that the

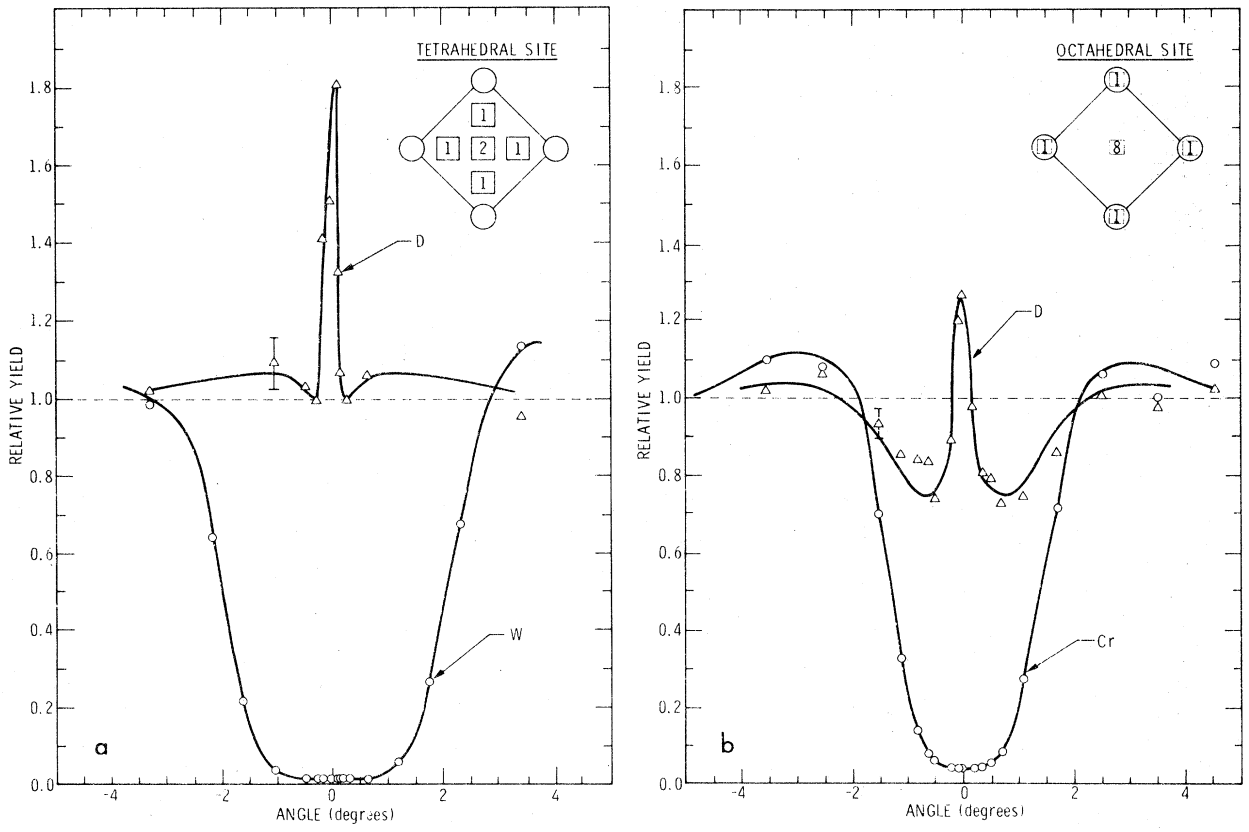

FIG. 1. Angular scans through the ⟨100⟩ axis for (a) W and (b) Cr for $3\times10^{15}/cm^2$ 30- and 15-keV D implants, respectively, at 296 K. A 750-keV ^3He analysis beam was used; circles correspond to backscattered yields for W and Cr, and triangles correspond to proton nuclear-reaction yields from D.

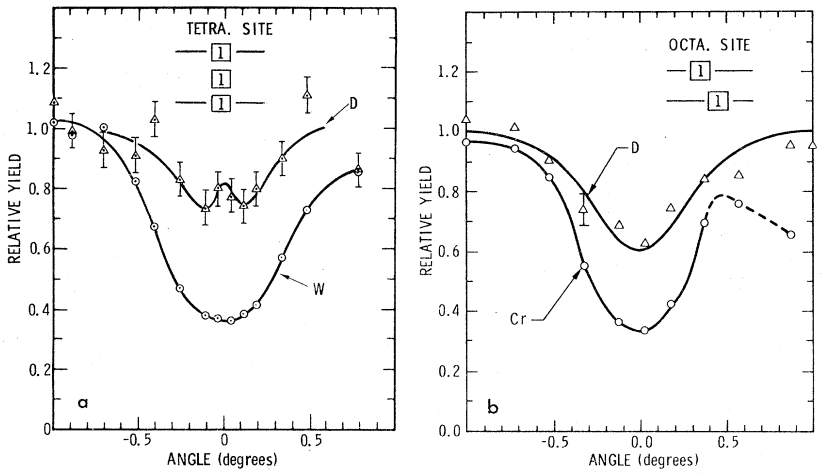

FIG. 2. Planar angular scans through the {100} plane for (a) W and (b) Cr with the same conditions as for Fig. 1.

D is in the tetrahedral interstitial site in W and in the octahedral interstitial site in Cr.

Schematic inset diagrams for a ⟨100⟩ projection of part of the unit cell show the locations and relative abundances of the two interstitial sites by the square boxes. The circles represent projections of the ⟨100⟩ lattice rows. None of the tetrahedral interstitial sites are shielded by metal atoms along the ⟨100⟩ lattice rows, whereas $\frac{1}{3}$ of the octahedral sites are. For D in Cr the broad D dip (yield ≈ 0.73) approaches the expected $\frac{1}{3}$ reduction (yield ≈ 0.67) with an angular width similar to that for the Cr lattice, in agreement with $\frac{1}{3}$ of the D atoms being along ⟨100⟩ lattice rows. Also the narrow central flux peak is consistent with $\frac{2}{3}$ of the D atoms in the center of ⟨100⟩ channels. In contrast a central flux peak with no dip is observed for W as expected.

Another important check on this interpretation is the data along the {100} plane shown in Fig. 2. Here $\frac{2}{3}$ of the tetrahedral sites lie in {100} planes and $\frac{1}{3}$ lie between the planes, whereas all of the octahedral sites lie within {100} planes. The data agree with the interpretation given in that D in W suggests a small flux peak superimposed on a dip, whereas the D in Cr exhibits only the dip. In addition, the planar D dip in W is $\frac{2}{3}$ of that in Cr.

From the magnitude of the D minimum yield in Cr for the ⟨100⟩ axis we conclude that $\gtrsim 82\%$ of the D atoms occupy octahedral interstitial sites. We need to consider also the additional data of the narrowness of the axial flux peaks and the increased yield and narrowing of the planar dips. The degree of D localization is given most accurately by the detailed shape of the dips. Increased vibrational amplitudes or slight displacements of the equilibrium position of impurities from shielded sites can lead to narrowing and increased yields of channeling dips. Considering the light mass of D, increased vibrational amplitude of the D relative to the lattice gives the simplest explanation of the data. Calculations based on the average-potential model indicate that quite large rms vibrational amplitudes, e.g., $\gtrsim 0.3$ Å in Cr, would be required to observe flux peak broadening; however, for D dips small amplitudes only slightly greater than that for the lattice, i.e., ≈ 0.11 Å for Cr, will result in smaller and narrower D dips. The observed D dips for the Cr and W {100} planes are both 60% smaller (± 10%) and, respectively, 10 and 20% narrower (± 15%) than the fraction of D atoms within the plane. No narrowing can be resolved for the ⟨100⟩ D dip in Cr but there is some evidence[5] that the ⟨100⟩ impurity width for the octahedral site can be wider than the host dip. Continuum-model estimates indicate that the planar data can be accounted for by D vibrational amplitudes of the order of 0.3 Å. This value is greater than the rms values of 0.16 Å in Cr and 0.14 Å in W predicted for D with the same force constants as the lattice atoms. The distance between octahedral and tetrahedral sites is 0.72 and 0.79 Å for Cr and W, respectively. Therefore, the axial data put severe constraints on multisite occupancy models which have been postulated[6] as possible for hydrogen in metals. For the present cases of Cr and W one of the two interstitial sites clearly dominates, in terms of the time-average spatial

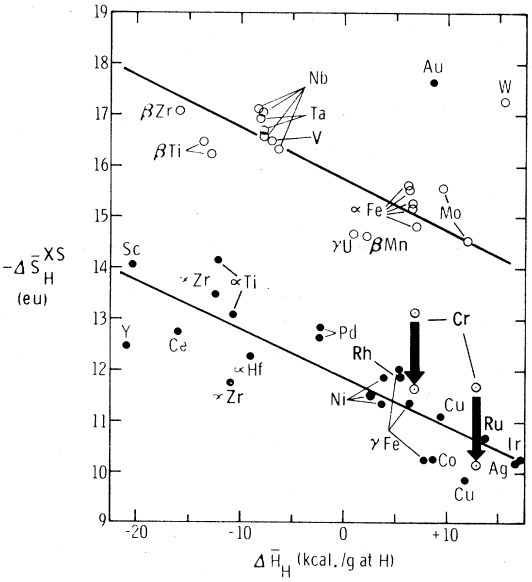

FIG. 3. Correlation between relative partial excess entropy, $\Delta\bar{S}_H^{XS}$, and relative partial enthalpy, $\Delta\bar{H}_H$, of ^{1}H in metals: open circles, bcc metals, closed circles, fcc and hcp metals. The data points for Cr at the top of the broad arrows were originally plotted in this figure from Refs. 3 and 8 based on tetrahedral site occupation. The values at the points of the broad arrows are the same data points using the new result of octahedral site occupation.

distribution.

We believe the octahedral position may also be the equilibrium position for dilute ^{1}H in Cr. An additional indication of the anomalous behavior of dilute ^{1}H in Cr relative to other bcc metals is given by ^{1}H solubility data. Gallagher and Oates[3] have observed the systematic trend reproduced in Fig. 3 which shows their plot of partial excess entropy $\Delta\bar{S}_H^{XS}$ and relative partial enthalpy (heat of solution) $\Delta\bar{H}_H$ of ^{1}H solution in the indicated metals. The open circles are bcc metals and the closed circles are the close-packed fcc and hcp metals. The plotted points were obtained from ^{1}H solubility versus T data using

$$RT\ln(p_{H_2}^{1/2}/X_H) = \Delta\bar{H}_H - T(\Delta\bar{S}_H^{XS} + R\ln\beta),$$

where X_H is the atom fraction of dissolved hydrogen, p the pressure of H_2 over the solid, R the gas constant, and β is the number of interstitial sites per metal atom. To obtain $\Delta\bar{S}_H^{XS}$ the configurational-entropy term, $R\ln\beta$, must be determined from lattice-location data. Gallagher and Oates[3] assumed the ^{1}H was located in tetrahedral sites in the bcc ($\beta=6$) and hcp ($\beta=2$) lattices and in octahedral sites in the fcc lattices ($\beta=1$).[7] (The ^{1}H lattice locations had not been measured for Cr and W.) We note that the Cr point originally plotted by Gallagher and Oates as well as a new point[8] at a lower $\Delta\bar{H}_H$ value (at the top of the broad arrows) both fall intermediately between the lines drawn through the bcc and the fcc/hcp data points. If we introduce our new information, which indicates hydrogen will occupy the octahedral interstitial site in bcc Cr($\beta=3$), the Cr points move down as shown by the arrows to group with the fcc metals where octahedral-site occupancy also predominates. The plotted point for W could possibly have large experimental uncertainties since data from several other investigators disagree markedly.[8,9]

The reason for the empirical thermodynamic correlation of Fig. 3 is not known. While reasonable differences in the vibrational contributions to the entropy[8] are consistent with the difference in magnitude ($\approx R\ln 6$) between the two lines, more vibrational data are necessary to explore this possibility. Based on our results for Cr it does not appear that the two lines result from a simple partition between the bcc and the closed-packed fcc and hcp metals.

Based on the implantation-channeling data and the empirical correlations in the thermodynamic results we suggest that hydrogen occupies the octahedral interstitial position in Cr and the tetrahedral interstitial position in W. The exact reason for this difference awaits a detailed electronic-structure calculation.

We gratefully acknowledge expert technical assistance by R. G. Swier.

†This work was supported by the U. S. Atomic Energy Commission.

[1]H. Fischer, R. Sizmann, and F. Bell, Z. Phys. 224, 135 (1969); H. D. Carstanjen and R. Sizmann, Phys. Lett. 40A, 93 (1972).

[2]S. T. Picraux and F. L. Vook, in *Applications of Ion Beams to Metals*, edited by S. T. Picraux, E. P. EerNisse, and F. L. Vook (Plenum, New York, 1974), p. 407.

[3]P. T. Gallagher and W. A. Oates, Trans. AIME 245, 179 (1969); R. B. McLellan and W. A. Oates, Acta. Met. 21, 181 (1973).

[4]D. K. Brice, private communication, and Radiat. Effects 6, 77 (1970).

[5]J. U. Andersen, E. Laegsgaard, and L. C. Feldman, Radiat. Effects 12, 219 (1972).

[6]A. M. Stoneham, Ber. Bunsenges. Phys. Chem. 76, 816 (1972).

[7]In the case of hcp Ru McLellan and Oates (Ref. 3) assumed octahedral site occupancy ($\beta = 1$) because of the low solubility of H in Ru and other similarities to Ni, Ir, and Rh.

[8]W. J. Arnoult and R. B. McLellan, Acta Met. 21, 1397 (1973). Note that the comment at the top of p. 1402 should read fcc instead of bcc and that the Cr point moves down in our Fig. 3 for octahedral site occupancy.

[9]R. Frauenfelder, J. Vac. Sci. Technol. 6, 388 (1969).

Optical Properties and Electronic Structure of Polymorphous TlCl and TlBr

K. Heidrich, W. Staude, and J. Treusch
University of Dortmund, 46 Dortmund-Hombruch, Germany

and

H. Overhof
University of Marburg, D-3350 Marburg, Germany

(Received 24 June 1974)

TlCl and TlBr can be forced to crystallize in the NaCl structure by evaporation on alkali-halide substrates, whereas they usually grow in the CsCl structure. Optical measurements on fcc layers of TlCl and TlBr are described for the first time. They are in good agreement with relativistic band-structure calculations, which are also reported in this Letter. An order-of-magnitude enhancement of exciton binding energies is explained as a consequence of a change in the type of chemical bond.

The optical properties of TlCl and TlBr have been a field of considerable experimental and theoretical interest over the past few years. Reliable optical-absorption data were published in 1970[1]; since then magnetoabsorption,[2] two-photon absorption,[3] stress optical,[4] and luminescence[5] measurements have been published. On the grounds of electronic band-structure calculations[6] the experimental data are well understood, special attention being paid to the exciton, which shows an unexpected low binding energy accompanied by a characteristic doublet structure.[4]

All the measurements reported above have been performed exclusively on single crystals or evaporated layers in the CsCl [simple cubic (sc)] structure. It has been known since 1951[7] that TlCl and TlBr can also crystallize in the NaCl (fcc) structure. These crystals are obtained by epitaxial growth on freshly cleaved crystals of a number of alkali halides, and are stable up to a size of about 200 Å. Thicker layers recrystallize in the sc structure.

Tutihasi[8] claimed to have measured the optical spectrum of fcc TlCl, which he prepared by evaporation on KCl. From the description of his experiments, which lack a structural analysis, we conclude that these layers were at least 1000 Å in thickness. For layers of these dimensions we found optical spectra similar to those of Tutihasi, which in the range from 3.5 to 4.2 eV do not exhibit any excitonic structure, whereas after annealing they show the typical excitonic spectrum of the sc structure. In the following we will demonstrate that the lack of any excitonic structure may be taken as a proof that neither fcc nor sc long-range order is present in layers of TlCl or TlBr.

We have evaporated TlCl and TlBr on several alkali-halide crystals at vacua of 10^{-5} Torr. The samples were then mounted into a cryostat attached to a Cary-17 spectrophotometer. Crystal structures were determined with an electron microscope.

Spectra taken at room temperature immediately after evaporation showed little dependence on the substrate material. Differences occurred after cooling as a result of the different thermal expansions of the substrates. In any case we found KBr to be suited best as a substrate, because it leads to layers which are least disturbed as compared to other substrates.

Figure 1 shows the absorption of sc and fcc TlCl and TlBr, respectively, on KBr substrates at 77 K. It can be seen that in thick layers there is still a certain amount of strain leading to an enlarged splitting of the first exciton line. Furthermore, this line is somewhat shifted to higher energies as compared with Fig. 1 of Ref. 1, and in the case of TlCl it is less well resolved. In spite of these effects, which are due to interactions